Soft Matter

Accepted Manuscript

ROYAL SOCIETY OF CHEMISTRY

www.rsc.org/softmatter

Convection Associated with Exclusion Zone Formation in Colloidal Suspensions

Sami Musa,[a,‡] **Daniel Florea,**[a,b,‡] **Hans M. Wyss,**[a,b,,*] **and Jacques Huyghe**[a,c,,*]

Received Xth XXXXXXXXXX 20XX, Accepted Xth XXXXXXXXX 20XX
First published on the web Xth XXXXXXXXXX 200X
DOI: 10.1039/b000000x

The long-range repulsion of colloids from various interfaces has been observed in a wide range of studies from different research disciplines. This so-called exclusion zone (EZ) formation occurs near surfaces such as hydrogels, polymers, or biological tissues. It was recently shown that the underlying physical mechanism leading to this long-range repulsion is a combination of ion-exchange at the interface, diffusion of ions, and diffusiophoresis of colloids in the resulting ion concentration gradients. In this paper, we show that the same ion concentration gradients that lead to exclusion zone formation also imply that diffusioosmosis near the walls of the sample cell must occur. This should lead to convective flow patterns that are directly associated with exclusion zone formation. We use multi-particle tracking to study the dynamics of particles during exclusion zone formation in detail, confirming that indeed two pronounced vortex-like convection rolls occur near the cell walls. These dramatic flow patterns persist for more than 4 hours, with the typical velocity decreasing as a function of time. We find that the flow velocity depends strongly on the surface properties of the sample cell walls, consistent with diffusioosmosis being the main physical mechanism that governs these convective flows.

1 Introduction

Exclusion zone formation (EZ formation) is a surprising effect where colloidal particles in a aqueous suspension are repelled from certain types of surfaces, leaving a particle-free zone near the surface. One of the remarkable properties of this EZ formation is the fact that it acts over distances much larger than the Debye length, which in water is limited to distances of around one micrometer. This length scale sets the range of electrostatic interactions - the longest-range direct interactions known to act on colloidal particles in a suspension.[1–3] This surprising EZ formation has been observed for various combinations of different surfaces and colloidal particles[4–9], always leading to the formation of a particle-free region near these surfaces. Depending on the field of study, the behavior has been referred to as aureole formation[8], formation of unstirred layers[6], or exclusion zone formation[4,5,7].
While various mechanisms have been proposed as the cause of this EZ formation[8,10–13], the physical origin has remained unclear. However, our recent experiments strongly suggest that exclusion zone formation is caused by a combination of ion-exchange at the surface, diffusion of ions, and diffusiophoresis of particles in the resulting ionic gradients[9]. In this physical picture, ion-exchange takes place at the active interface, where cations present in the solution are exchanged for H^+-ions of higher mobility, which leads to the build-up of a gradient in the ion concentration in the suspension. This ion-gradient in turn causes the colloidal particles in the suspension to move away from the active surface via so-called diffusiophoresis, the migration of particles in a liquid, driven by a gradient in ion concentration.

In this paper, we present a new physical characteristic associated with exclusion zone formation, which - to our knowledge - has not previously been reported. Using Nafion, for which EZ formation has been extensively studied, in contact with suspensions of polystyrene colloids, we observe substantial convective flows that accompany EZ formation. We characterize these flows in detail using microscopy and multi-particle tracking techniques. As shown in our previous study[9], diffusiophoresis occurs in the system due to a concentration gradient that is caused by an ion-exchange between the Nafion and the aqueous solution. Besides driving the EZ formation itself, we hypothesize that the same concentration gradients also cause the observed convective flows in our system. In our earlier study, we were able to suppress convective flows via buoyancy forces, by placing the sample cells in a vertical orientation with the active surface at the top; this strategy

† Electronic Supplementary Information (ESI) available: (details of any supplementary information available should be included here). See DOI: 10.1039/b000000x/

[a] *Department of Mechanical Engineering, Materials Technology, Eindhoven University of Technology, Eindhoven, the Netherlands*
[b] *Institute for Complex Molecular Systems, Materials Technology, Eindhoven University of Technology, Eindhoven, the Netherlands*
[c] *Bernal Institute, University of Limerick, Limerick, Ireland*
* To whom correspondence should be addressed at H.M.Wyss@tue.nl, and J.M.R.Huyghe@tue.nl.
‡ These authors contributed equally to this work.

efficiently suppressed convective flows within and near the exclusion zone region, irrespective of the physical origin of these flows. In contrast, for a horizontal sample cell orientation, as studied here, we always observe significant convective flows. Nevertheless, while gravity itself clearly also can drive convective flows, as evidenced by violent Rayleigh-Taylor like instabilities observed in vertical cells with Nafion at the bottom, we do not expect gravity to play a large role when the cells are oriented in a horizontal position. Instead, we hypothesize here that the main physical mechanism responsible for these flows is the so-called diffusioosmosis effect[14–16], which drives a flow of fluid along a charged surface, induced by a salt concentration gradient. The same salt concentration gradients that drive EZ formation should thus lead to a flow of the background fluid along the glass side walls of the sample chamber, resulting in convective flows in the system.

Indeed, we find that the systematic dependence of the flow velocity on the surface potential of the cell walls is consistent with our hypothesis of diffusioosmosis as a driving force for these flows. A full description of EZ formation thus has to take into account the diffusioosmotic effects we have studied here, as the convective flows occurring due to diffusioosmosis also influence EZ formation. Accounting for the complex interplay of diffusiophoretic and diffusioosmotic driving forces will be beneficial for the broad range of research fields where the phenomenon of EZ formation is important. Understanding and predicting these flows is of essential importance in new technologies that make direct use of exclusion zone formation, for instance for separation technologies or for water purification.

2 Experimental

To quantify the flow patterns associated with the formation of exclusion zones we have conducted multi-particle tracking experiments using time-resolved optical microscopy, combined with digital image analysis.[17] This allows us to precisely determine the flow velocity profile within our samples. The samples used in the experiments consist of an ion-exchange polymer thin film immersed in an aqueous suspension of microparticles. As the polymer film we have used a Nafion membrane (Nafion® 117, Sigma-Aldrich, USA), which is an ion-exchange polymer comprising a Teflon backbone with perfluoride side chains containing a sulfonic acid group. The Nafion film has a thickness of 170 μm and 200 μm, in a dry and wet state, respectively. The Nafion film was rinsed in deionized water for 30 minutes before being placed in the sample cells. In all experiments the concentration of micro-beads in the suspension was maintained at 0.04 wt%. Also, in the preparation of all samples we have used deionized water (Milli-Q water, $\sigma > 18\mathrm{M}\Omega \cdot \mathrm{cm}$ at 25 C). There were no additional salts or other substances added to the suspension. However, the supplied polystyrene particles used in our experiments are supplied in an aqueous buffer solution which contains around 1% of surfactant and inorganic salts, including 0.2 wt% sodium bicarbonate and potassium sulfate. Thus, after dilution with deionized water the salt concentration in the final suspension is $\approx 3 \cdot 10^{-5}$ moles/liter.[18]

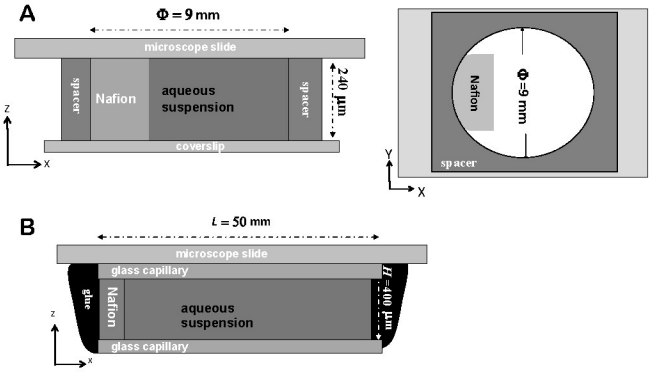

Fig. 1 Schematic illustration of the sample cells used in the experiments. (A) Left: Cross-section view of *sample cell type A* where the sample is placed between a microscope slide and a coverslip separated by a 240 μm spacer. The Nafion film is attached to the sticky spacer. Right: Top-down view of *sample cell type A*. The cell is a 9 mm-diameter well, bounded by the spacer. **(B)** Cross-section view of *sample cell type B*, which consists of a capillary tube (L = 50 mm x W = 4 mm x H = 0.4 mm) glued to a microscope slide. The Nafion membrane is fitted to one side of the tube and the suspension is filled in from the other side, prior to sealing with 5-minute epoxy.

In the experiments two configurations of sample chambers/cells were used. Fig.1(A) depicts a top and a cross section view of sample cell type A. The chamber was formed by sandwiching a 240 μm spacer between a microscope slide and a coverslip; it has a diameter of 9 mm. Sample cell type B, schematically shown in Fig.1(B), consists of a glass capillary tube (Vitrocom) with a length of 50 mm, width of 4 mm, and height of 0.4 mm. This tube was fitted at one end with Nafion by stamping the tube for 20 seconds on a Nafion sheet, which was pre-heated on a microscope cover slide to 265 °C. This process ensures that the Nafion material fills the capillary uniformly, thereby completely sealing it. In addition, around the connection area between the Nafion and the glass, the cells were sealed using a UV curable epoxy glue (Norland NOA63) to prevent evaporation. Finally, after placing the colloidal suspension into the cell, the other end of the cell was sealed with a 5-minute epoxy glue (5 minute epoxy, Bison).

The aqueous particle suspensions contain polystyrene microbeads with a diameter of 1 μm (Polyscience Inc., USA). The particles are negatively charged in aqueous suspension; we determine the zeta potential of the particles as $\zeta \approx -55\,\mathrm{mV}$ using electrophoretic light scattering (Zetasizer, Malvern In-

struments LTD, UK. pH 7, 1mM NaCl solution).

Immediately prior to each measurement, the sample cells were filled with this aqueous particle suspension. To avoid bubble formation during filling, we tilted the capillary such that its largest dimension was oriented vertically. With a modified Pasteur pipette that was pulled in a flame in order to create a long microneedle, the sample was injected slowly into the cell near the Nafion surface, thus moving the fluid from near the surface up towards the end of the capillary and circumventing the entrapment of bubbles.

Multi-particle tracking measurements were performed using an inverted microscope (Axiovert 200M, Zeiss, Jena, Germany). Videos of flowing micro-beads were acquired using an attached CCD camera (The Imaging Source, Charlotte, NC, USA) with a maximum frame rate of 60 frames/second and a resolution of 640 x 480 pixels. In recording the videos we have used a 40x microscope objective (Zeiss, NA=0.5). The recorded videos were analyzed using a particle tracking protocol described by Crocker et al.[17], where images are processed using a bandpass filter and potential particle positions are determined as local maxima in each image; features not corresponding to tracer particles are discarded using criteria such as the size, intensity, or aspect ratio of the detected feature. The resulting particle positions obtained in different frames were then connected to reconstruct the trajectories of the individual particles. The resulting trajectories could then be used to calculate the mean drift velocity of the particles.

Error analysis for measured drift velocities: To minimize the measurement errors in determining drift velocities from this particle tracking procedure, we checked for pixel biasing on our measurements and ensured that we can reach a subpixel resolution in the measurements, as described by Crocker et al. [17].

In accordance with this we estimate the error of an individual position measurement as +- 13 nm, as in our setup one pixel on the camera corresponds to a length scale of ≈ 120 nm and one particle thus corresponds to around 9 pixels. We therefore expect to reach an accuracy of $120\ \mathrm{nm}/9 \approx 13$ nm. In addition, there is an inherent error in measuring drift velocities as a result of the random Brownian motion of the particles: Estimating the diffusion coefficient of our polystyrene particles from the Stokes-Einstein equation, we obtain $D \approx 4 \cdot 10^{-9}\mathrm{cm}^2/\mathrm{s}$. Between two frames, the colloidal particles are thus expected to move by Brownian motion by a typical distance of $\sqrt{(D \cdot \Delta t)}$,with Δt the time interval between two frames. This yields a value of $\approx 8 \cdot 10^{-6}$ cm $= 8$ nm, which is comparable to the position accuracy of the particle tracking method. In each frame we typically have at least $N \approx 100$ particles present that can be successfully tracked. Averaging over all these particles leads to a $\sqrt{N}$-fold reduction in the error for recording the drift velocity, yielding a total error for the center of mass position between two frames on the order of ~ 2 nm. These errors are further reduced by averaging over a large number of position measurements, taken at different points in time. We recorded for at least 60 seconds at 60 frames/second, yielding 3600 measuring points. In conclusion, the errors on the drift velocities are very small, even when neglecting the averaging over a large number of position measurements, we estimate an error for the measured drift velocities on the order of $\Delta v \approx \frac{2\ \mathrm{nm}}{1/60\ \mathrm{s}} \approx 0.1\ \mu\mathrm{m/s}$.

3 Theoretical background

We hypothesize that the so-called diffusioosmosis effect plays a key role in driving the complex flow patterns that are observed in exclusion zone formation experiments. We will therefore in the following give some theoretical background on this phenomenon. Diffusioosmosis takes place when a solution exhibiting a solute concentration gradient is in contact with a charged surface[14]. The effect generates flows parallel to the charged surface through two physical mechanisms: The first mechanism, referred to as chemio-osmosis, occurs as a result of the solute concentration gradient creating an osmotic pressure gradient in the double layer along the charged surface. This unbalanced osmotic pressure in turn drives fluid flow parallel to the surface. The second mechanism is an electro-osmosis effect, driven by a concentration gradient: The concentration gradient establishes an electric field to balance the diffusion current and prevents the oppositely charged ions of the electrolyte from drifting apart. This electric field drives the counter-ions in the diffuse layer next to the surface and consequently causes fluid flow. The diffusioosmotic flow velocity at distances beyond the Debye length, which is the regime relevant to our measurements, can be approximated as[14]

$$\frac{U_\infty}{U^\star} \approx \beta \frac{Ze\zeta}{k_\mathrm{B}} + 4 \ln \cosh\left(\frac{Ze\zeta}{4k_\mathrm{B}T}\right) \qquad (1)$$

where $\frac{U_\infty}{U^\star}$ is the bulk fluid flow velocity normalized by a typical diffusioosmotic velocity,

$$U^\star = \left(\frac{2k_\mathrm{B}T}{\eta\kappa^2}\right)|\nabla C_\infty| \propto \frac{\nabla C_\infty}{C_\infty} = \nabla(\log(C_\infty)), \qquad (2)$$

with Z the valence of the ions of the electrolyte, e the proton charge, ζ the zeta potential, β the difference between diffusivities of the counter- and co-ions normalized by their sum, k_B the Boltzmann constant, T the absolute temperature, κ the inverse Debye screening length, η the fluid viscosity, and C_∞ the solute concentration in the bulk solution. The first term in Eq.1 accounts for the electro-osmotic effect, while the second term gives the chemio-osmotic component. Eq.1 thus predicts a monotonic increase of the fluid flow velocity with increasing zeta potential. It is important to note that Eq.1 describes an

idealized situation where the surface is infinitely extended and where the ion concentration gradient remains constant along this surface. However, in our case, the gradient of salt concentration varies significantly along the wall surface, being strongest at the Nafion surface. As the different regions along the surface are hydrodynamically coupled, the fluid velocity at a certain point on the surface is expected to not depend only on the gradient of salt concentration exactly at that point, but also on the salt gradient in neighbouring regions. This is in contrast to the diffusiophoresis effect, where the particle motion relative to the fluid depends only on the ionic gradients in the immediate vicinity of the particle.

A remarkable property of both diffusiophoresis and diffusioosmosis is that the magnitude of the associated slip velocities depends on the relative, rather than the absolute value of the ionic gradient present in the solution, as $U \propto \nabla(\log C) = \nabla C/C$; this means that even though they rely on ionic gradients in the background solution, these effects operate even at very low ionic concentrations, such as for the suspensions studied here.

The effects of diffusioosmosis, driving fluid flow, and diffusiophoresis, driving the migration of particles within the fluid, are intimately related; in fact, they have the same physical origin. The diffusiophoresis of particles can be regarded as a diffusioosmosis effect that takes place at the surface of the particles, resulting in a displacement of the fluid relative to the particle surface. As both the fluid and the particle are incompressible, the net result is a motion of the particles in the opposite direction, generally towards regions of higher salt concentration.

As a result of this analogy, the particle drift velocity due to diffusiophoresis is equal to the negative of the velocity of the diffusioosmotic flow given by Eq.1, with the corresponding surface properties replaced by those of the suspended particles.

In our experimental system we expect that besides diffusiophoresis, acting on the suspended particles, diffusioosmosis, acting on the fluid near the cell walls, should also occur, as we expect the glass walls of both type A and B cells to become charged when coming in contact with water. Glass acquires charges because silanol groups, SiOH, on its surface dissociate in water. In this process protons, H^+, are released and the glass surface becomes negatively charged, forming an electrical double layer[19].

4 Results and Discussion

To test our hypothesis of diffusioosmosis driving convection in our system, we perform dedicated experiments to study the occurring flows in detail. In agreement with previous studies, in all our experiments we observed that upon exposure of a piece of Nafion to a colloidal suspension, the colloidal particles move away from the Nafion surface. As a consequence of this motion, a colloid-free exclusion zone develops near the Nafion film. Ion-exchange between the Nafion and the surrounding solution leads to a solute concentration gradient in the solution next to the Nafion. This concentration gradient evolves as a function of time due to the diffusion of the different species of ions in the solution. In turn, the presence of this ion concentration gradient generates a directed motion of particles away from the Nafion surface.[9]

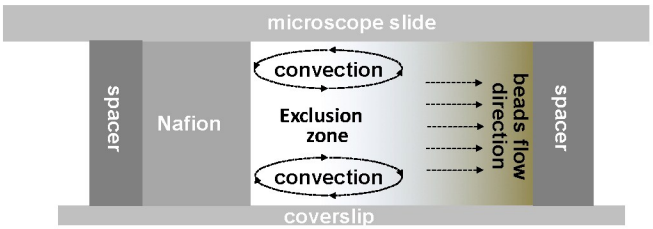

Fig. 2 Schematic of EZ formation and associated convective flows. The gradient in ionic concentration within the cell is schematically shown as a gradient in brightness; darker colors represent higher ionic concentrations.

However, we also observe phenomena that cannot be fully accounted for solely by diffusiophoretic forces acting on the particles. Namely, we observe a surprising reversed motion of a sub-population of particles; these particles flow rapidly in the direction opposite to that of EZ formation, back towards the Nafion. Interestingly, such reverse flows only occur at the top and bottom sides of the cell, near the cell walls, as shown schematically in Fig.2. As the beads approach the Nafion film they change direction to first move parallel to the Nafion surface and finally to propagate away from it. This movement creates two vortex-like convection rolls near the upper and lower regions of the cell.

This phenomenon can be observed even without detailed particle velocity measurements, as seen in Fig.3, where we show a top view optical microscope image of a piece of Nafion immersed in an aqueous suspension of 1-μm-diameter polystyrene beads. Within the main exclusion zone, a narrow dark strip near the Nafion is clearly visible; we interpret this feature in agreement with the observed convection rolls. Seen from atop, such convection rolls should indeed appear darker near the Nafion, as here the layer of particles in the roll is oriented perpendicular to the field of view.

To study these convection rolls in detail, we record videos of the movements of the beads in imaging planes parallel to the horizontal cell walls, using optical microscopy. These captured imaging planes are separated by 5 μm in the $z-$direction and are 76.8 μm long and 57.6 μm wide, along the $x-$ and $y-$axis, respectively. Along the $x-$axis they are 40 μm from the Nafion surface, and they are situated in the middle of the cell along the $y-$axis.

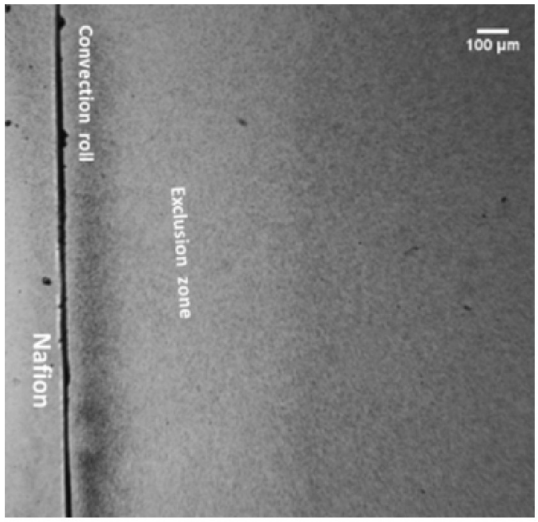

Fig. 3 Top view optical microscope image showing the edge of a Nafion film, the exclusion zone, and a convection roll, which appears as a dark line close to the Nafion film.

In both cells of type A and type B, the same general behavior is observed, as shown in Fig.4(a) and Fig.4(b), respectively, where we plot the average lateral velocity as a function of distance from the bottom cell wall. In both cells we find that this average velocity is highest near the upper and lower cell walls and decreases towards zero with increasing distance from the cell wall. At even longer distances from the walls, the beads reverse their direction, now moving away from the Nafion surface. These flow patterns are consistent with rotational vortex flows where the speed increases as a function of the distance from the center of the vortex. The shape of the flow profiles for cells of different heights (240 μm for cell type A and 400 μm for cell type B) is surprisingly similar; the shapes essentially scale on top of each other when rescaling the heights, as can be seen by comparing Fig.4(A) and Fig.4(B).
Moreover, we observe that for both cell types the flow velocities in the upper vortex are slightly higher than in the lower vortex. These differences can be partly accounted for by the fact that measurements in the different planes are not performed at the same time. A full measurement, starting at the top of the cell and ending at the bottom, takes typically one hour. The observed differences between the two rolls could thus be related to the fact that we cannot simultaneously measure the flow velocities across the entire cell.

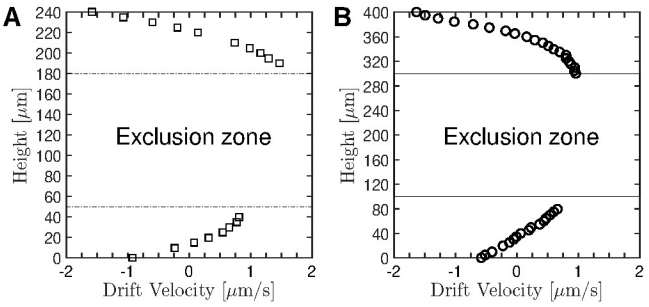

Fig. 4 Velocity profiles obtained from particle tracking. Average drift velocities obtained from particle trajectories extracted from microscopy images taken in planes parallel to the top and bottom cell walls. The $y-$axes are the distance from the bottom of a sample cell of *type A* (A) and *type B* (B), respectively. The estimated error in detecting the drift velocities is $\approx 0.1\mu$m/s, smaller than the symbols used in these plots.

To test for such a potential time-dependence, we follow the average flow velocity at a fixed distance from the cell wall as a function of time, shown in Fig.5. This measurement is performed in a plane located 15 μm from the bottom of a type B cell. The recording is repeated every 5 minutes during more than 4 hours. We observe a gradual decrease of the average flow velocity, from ~ 0.5 μm/s at the start of the measurement to ~ 0.35 μm/s after four hours. Indeed, considering only diffusion, we would expect the concentration gradient at a fixed position to decrease with time t as $\propto 1/\sqrt{(t)}$. However, due to the complex interplay of diffusion and convective flows in our system, the exact functional form is difficult to predict. In summary, if not suppressed by buoyancy forces, the observed flow patterns appear to be a robust feature accompanying exclusion zone formation; we have observed essentially the same behavior in different cell types. We have further shown that the convective flows, while time-dependent, are sustained for more than 4 hours.

While these observations are in agreement with our hypothesis of diffusioosmosis driving the observed convective flows, they are still not fully conclusive. For instance, as the zeta potential of our particles is similar to that of the glass side walls, based on Eq.1 we would at first sight not expect particles located near the cell side walls to move considerably, as one would expect the diffusiophoretic migration of particles relative to the fluid, away from the Nafion surface, to be ap-

proximately matched by a overall diffusioosmotic flow of the fluid in the opposite direction. However, as pointed out above, for the case of diffusioosmosis Eq.1 strictly applies only if the ion concentration gradients along the surface are uniform; in our setup this is not the case and hydrodynamic coupling between different regions will affect the actually observed particle velocities. This is only one example of the expected complex interplay of convective flows, diffusiophoresis, and diffusioosmosis, which makes it difficult to predict the detailed flows in the system and to directly test our hypothesis of diffusioosmosis having a large role in driving convective flows in or system. However, it is possible to tune the magnitude of diffusioosmotic flows independent of the other physical effects at hand, thereby directly probing their relative importance in contributing to the observed overall flow patterns.

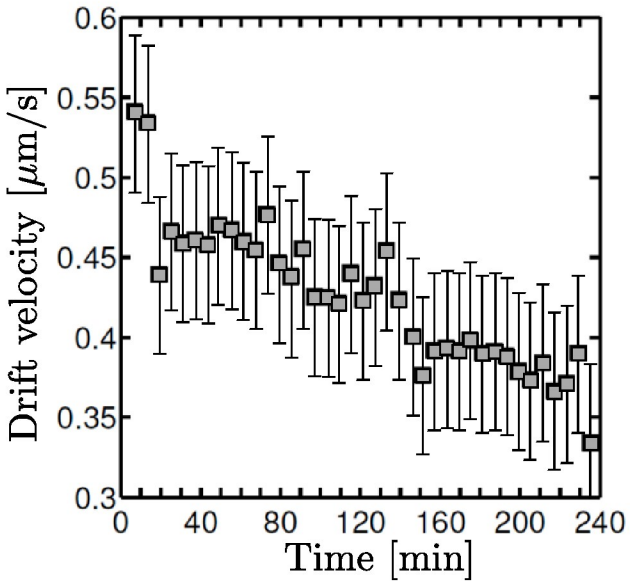

Fig. 5 Time dependence of the average bead velocity. The measurement was performed in a plane that is separated by 15 μm from the bottom of a type B cell. The estimated error in detecting the drift velocities is $\approx 0.1\mu$m/s, as indicated by the error bars.

To do so, we perform experiments in which we significantly change the surface properties of the cell walls. If indeed diffusioosmosis contributes significantly to the observed convective flows, marked differences in flow velocity should be observed. To achieve such a change in surface properties, we coat the microscope slide and the coverslip of a type A cell with a 20 nm-thick gold layer using a sputter coater (Emitech K575X Turbo Sputter Coater). Previous studies have found that such a gold-coated surface exhibits a significantly lower zeta potential compared to uncoated glass; for instance, the zeta potential for gold and glass were measured as –20 mV and –67 mV, respectively, at pH = 6 and ionic strength of 10^{-3} M [20]. These differences should lead to significantly different diffusioosmotic flow velocities, which can be estimated using Eq.1. Using the above values for the zeta potentials of glass and gold surfaces, and an expected range of ion diffusivity contrasts of $-1 < \beta < -0.2$, we predict a value of between 4.1 and 5.7 for the ratio of the flow velocities in cells with uncoated and gold-coated surfaces, respectively.

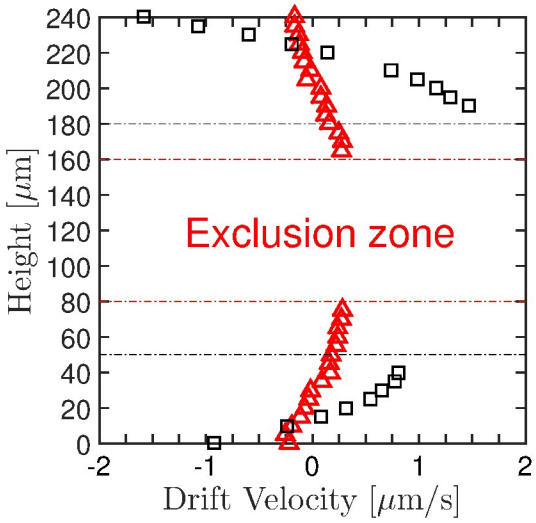

Fig. 6 Influence of cell wall surface properties. Average flow velocities measured in a cell of type A with uncoated (black squares) and gold-coated (red triangles) glass cell walls. In both cases two convection rolls are observed near the cell walls; the typical velocities in the presence of gold-coated cell walls are significantly lower than for the untreated glass surfaces. The estimated error in detecting the drift velocities is $\approx 0.1\mu$m/s, smaller than the symbols used in this plot.

Indeed, our experiments are consistent with this prediction, as shown in Fig.6, where we compare the flow behavior in cell of type A with uncoated and gold-coated surfaces, respectively. We observe significantly lower flow velocities for the gold-coated case compared to those measured in a cell with untreated glass surfaces. For the untreated case, the average flow velocity towards the Nafion surface near the cell walls is $0.62\mu m/s$; the corresponding average velocity for the gold-coated case $0.11\mu m/s$. Within experimental error, our measurements are thus consistent with the above estimates of the expected differences in flow velocity, based on Eq.1. This further confirms that our results are consistent with diffusioosmosis as the mechanism driving the observed convective flows.

5 Conclusions

We have performed a systematic experimental study of flow patterns arising during exclusion-zone formation, which occurs when a colloidal suspension is exposed to an ion-exchanging surface. It has recently been shown that the physical origin of such exclusion-zone formation is a combination of ion-exchange, diffusion of ions, and diffusiophoresis of colloidal particles in the resulting time-dependent ionic gradients. However, the effects of other surfaces in the system, such as the walls of the sample chamber, have previously been neglected.

By studying the developing flow patterns in detail via multi-particle tracking, we have observed that exclusion zone formation is accompanied by convective flows, which in our systems appear as double convection rolls. Our results provide a quantitative description of the flow velocity profile across these convection rolls. They also show that these flows can be maintained for a period of more than 4 hours and that their velocity decreases as a function of time. The results of our study of these flow patterns clearly indicate that diffusioosmosis, in addition to diffusiophoresis, contributes significantly to the flow of fluid and particles in exclusion zone formation. Further strengthening this hypothesis we show that the flow velocity is dependent on the surface charge of the cell walls, consistent with the behavior expected for diffusioosmotic flow. A full description of the complex flow patterns occuring during exclusion zone formation thus requires taking into account the complex interplay between diffusiophoresis, which drives particle motion relative to the background fluid, as well as diffusioosmosis at the cell walls, which drives convective flows of the fluid. The observed pronounced flow patterns that accompany exclusion zone formation in these systems could be exploited for mixing of fluids in microfluidic devices or for other applications where a precise control of fluid flows at small length scales is required.

6 Acknowledgements

Sami Musa gratefully acknowledges financial support from the Technology Foundation STW, the technological branch of the Netherlands Organization of Scientific Research, NWO, and the Dutch ministry of Economic Affairs under contract 12538 Interfacial effects in ionized media. D.F. And H.M.W. are grateful for financial support from the ICMS at Eindhoven University of Technology. We thank Audrey Champion (Department of Mechanical Engineering, Eindhoven University of Technology) for depositing the gold layers.

References

1 B. V. Derjaguin and L. Landau, *Acta Phys. Chim. URSS*, 1941, **14**, 633–662.
2 E. J. W. Vervey and J. T. G. Overbeek, *Theory of the Stability of Lyophobic Colloids*, Elsevier Publishing Company Inc., Amsterdam, 1948.
3 A. V. Delgado, F. González-Caballero, R. J. Hunter, L. K. Koopal and J. Lyklema, *Pure and Applied Chemistry*, 2005, **77**, 1753–1805.
4 J.-M. Zheng and G. H. Pollack, *Phys. Rev. E*, 2003, **68**, 031408.
5 J. M. Zheng, W. C. Chin, E. Khijniak and G. H. Pollack, *Advances in Colloid and Interface Science*, 2006, **127**, 19–27.
6 K. Green and T. Otori, *The Journal of Physiology*, 1970, **468**, 93–102.
7 B. Chai, A. G. Mahtani and G. H. Pollack, *Contemporary Materials*, 2012, **1**, 21–22.
8 B. V. Deryagin and M. V. Golovanov, *Colloid Journal of the USSR*, 1986, **48**, 209–211.
9 D. Florea, S. Musa, J. M. R. Huyghe and H. M. Wyss, *PNAS*, 2014, **111**, 6554–6559.
10 E. Del Giudice, A. Tedeschi, G. Vitiello and V. Voeikov, *J. Phys.: Conf. Ser.*, 2013, **442**, 012028.
11 J. M. Schurr, B. S. Fujimoto, L. Huynh and D. T. Chiu, *The Journal of Physical Chemistry B*, 2013.
12 J. M. Schurr, *The Journal of Physical Chemistry B*, 2013.
13 G. H. Pollack, *J Phys Chem B*, 2013, **117**, 7843–7846.
14 H. J. Keh and H. C. Ma, *Langmuir*, 2005, **21**, 5461–5467.
15 H.-F. Huang, *Colloids and Surfaces A: Physicochemical and Engineering Aspects*, 2011, **392**, 25–37.
16 S. Qian, B. Das and X. Luo, *J. Colloid Interf. Sci.*, 2007, **315**, 721–730.
17 J. C. Crocker and D. G. Grier, *J. Colloid Interf. Sci.*, 1996, **179**, 298–310.
18 *Sigma Aldrich Product Information for Polystyrene Latex Beads, Sigma Prod. Nos. LB-1, LB-3, LB-5, LB-6, LB-8, LB-11, LB-30, LB-120, SD-6A, SD-26, SD-91, CLB-4, and CLB-9. www.sigma-aldrich.com.*
19 S. H. Behrens and D. G. Grier, *J Chem Phys*, 2001, **115**, 6716–6721.
20 M. Giesbers, J. M. Kleijn and M. A. Cohen Stuart, *J. Colloid Interf. Sci.*, 2002, **248**, 88–95.

Text for table of contents entry

Our experiments on exclusion-zone formation in colloidal suspensions indicate that in addition to diffusiophoresis of the particles, diffusioosmotic flows of the fluid play an important role and lead to double convective flow patterns.